

Supporting Information

Reactions of a sulfonamide antimicrobial with model humic constituents: Assessing pathways and stability of covalent bonding

*Anna Gulkowska^{†, ‡}, Martin Krauss^{§, †, *}, Daniel Rentsch[#], Juliane Hollender^{†, ‡}*

[†]Eawag, Swiss Federal Institute of Aquatic Science and Technology, 8600 Dübendorf, Switzerland

[‡]Institute of Biogeochemistry and Pollutant Dynamics (IBP), ETH Zürich, 8092 Zürich, Switzerland

[§]Department Effect-Directed Analysis, UFZ - Helmholtz Centre for Environmental Research, 04318 Leipzig, Germany

[#]Empa, Swiss Federal Institute for Materials Science and Technology, 8600 Dübendorf, Switzerland

*Corresponding author:

tel. 0049-341 235 1530, fax. 0041-341 235 451530, email: martin.krauss@ufz.de

Number of pages: 23

Number of tables: 2

Number of figures: 10

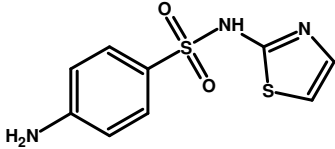
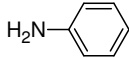
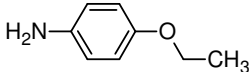
Materials and Methods

Chemicals. Sulfathiazole (STZ) (4-amino-*N*-(2-thiazolyl)-benzenesulfonamide, Sigma-Aldrich, St. Louis, MO), sulfamethazine (SMZ) (4-amino-*N*-(4,6-dimethyl-2-pyrimidinyl)-benzenesulfonamide), aniline (ANL) (Sigma-Aldrich), and *p*-ethoxyaniline (EXA) (for synthesis, Merck, Darmstadt, Germany) were used as received. For NMR studies ¹⁵N aniline (98 atom % ¹⁵N) was bought from Isotec (Miamisburg, OH).

The model phenols catechol (CAT) (1,2-dihydroxybenzene, purity > 99%), 4-methylcatechol (4-mCAT) (3,4-dihydroxytoluene, 95%), protocatechuic acid (PRO) (3,4-dihydroxybenzoic acid), gentisic acid (GEN) (2,5-dihydroxybenzoic acid), acetosyringone (AcSYR) (4-hydroxy-3,5-dimethoxyacetophenone, 97%), *trans*-ferulic acid (FER) (*trans*-4-hydroxy-3-methoxycinnamic acid, 99%), esculetin (ESC) (6,7-dihydroxycoumarin, 98%), syringic acid (SYR) (4-hydroxy-3,5-dimethoxybenzoic acid, 98%), hydroquinone (HQ), and *p*-benzoquinone (BQ) were purchased from Sigma-Aldrich, and vanillic acid (VAN) (4-hydroxy-3-methoxybenzoic acid) was obtained from Alfa Aesar (Karlsruhe, Germany). The model non-quinone carbonyl compounds 1-penten-3-one, acetylsalicylic acid, acetic acid *p*-tolyl ester, methyl benzoylformate, and 1-phenyl-1,2-propanedione with purities ranging between 98 and 99.5 % were purchased from Sigma-Aldrich (Buchs, Switzerland). Individual stock solutions for all compounds were prepared in methanol with concentrations of 1 mg/mL.

HPLC grade methanol, acetonitrile and water (Acros Organics, Geel, Belgium) were used as solvents for extraction and as liquid chromatography eluents. Ammonium acetate, formic acid, acetic acid, and tris(hydroxymethyl)aminomethane (Tris) of “pro analysi” grade were obtained from Merck.

Table S1. Chemical structures of sulfathiazole and other model aromatic amines used. The anticipated nucleophilic reactivity is given relative to each other (+ = lowest, +++ = highest).

Compound	Structure	Nucleophilic reactivity of amino group ^a
4-Amino-N-(2-thiazolyl)-benzenesulfonamide (Sulfathiazole, STZ)		+ pK _a = 2.30
Aminobenzene (Aniline, ANL)		++ pK _a = 4.60
1-Amino-4-ethoxybenzene (Ethoxyaniline, EXA)		+++ pK _a = 5.36

^a The assumed nucleophilic reactivity is based on pK_a values taken from Richter *et al.*¹ for STZ and EXA and from Mackay *et al.*² for ANL, as the pK_a of the conjugate acid of the nucleophile and the rate of the reaction can be described by a Brønsted linear free energy relationship³ if the donor atom of all nucleophiles is similar and the same solvent is used.

LC-MS/MS analysis of aromatic amines. The LC-MS/MS system consisted of an autosampler (HTC PAL, CTC Analytics, Zwingen, Switzerland), a Rheos 2000 LC pumps (Flux Instruments, Basel, Switzerland), a column oven (Jones, Omnilab, Mettmenstetten, Switzerland), and a triple quadrupole mass spectrometer with an electrospray probe (TSQ Quantum, Thermo Finnigan, San Jose, CA). 20 μL of samples were injected and separated at a flow rate of 200 $\mu\text{L}/\text{min}$ using a Nucleodur C18 Gravity column (125 mm \times 2 mm, 5 μm particle size; Marcherey-Nagel, Oensingen, Switzerland) equipped with a guard column by gradient elution. The mobile phases consisted of water (A) and methanol (B), both containing 0.1% of formic acid. The composition of the mobile phase was changed linearly from 5% B at the start to 95% B at 14 min before re-equilibration to starting conditions.

The mass spectrometer was operated in full scan mode with a range of m/z 80-800 and selected reaction monitoring (SRM) mode with the following electrospray ionization (ESI) conditions: positive mode, spray voltage 3500 V, sheath gas pressure 4 MPa, auxiliary gas pressure 0.5 MPa, ion transfer capillary temperature 350°C.

The error of the analytical procedure was below 10%. External calibration curves of ten concentrations (2-1500 ng/mL) were measured for the quantification of the analytes in the samples. Quality control standards were measured after every 10 injections to check for instrumental drift. The analysis was stopped and a new calibration curve was constructed if the quality control standard was not within $\pm 10\%$ of its theoretical value. Details on detection limits and recovery rates were published elsewhere.¹ Instrumental blank samples consisting of water/methanol 90:10 (v/v) were run to check for analyte carryover.

^1H and ^{15}N NMR analysis of ^{15}N aniline reactions products with CAT and SYR. The ^1H and ^{15}N NMR spectra were recorded at 400.13 (40.56) MHz on a Bruker Avance-400 NMR spectrometer (Bruker Biospin AG, Fällanden, Switzerland). The 1D ^1H and 2D ^1H - ^{15}N HMBC correlation experiments were performed at 298 K using a 5 mm broadband inverse probe with z-gradient (100% gradient strength of 53.5 Gcm^{-1}) and 90° pulse lengths of 6.8 μs (^1H) and 20.7 μs (^{15}N). All NMR spectra were recorded with the Bruker standard pulse programs and parameter sets with selection of coupling constants of 4 Hz (gs-HMBC). The ^1H chemical shifts in water were referenced to an external sample of 3-trimethylsilyl tetradeutero sodium propionate in D_2O at 0.0 ppm and the ^{15}N chemical shifts were internally referenced to the signal of aniline at 58.0 ppm with respect to the NH_3 chemical shift scale with δ (^{15}N) = 0.0 ppm.⁴

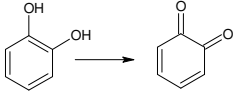
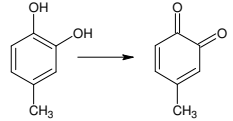
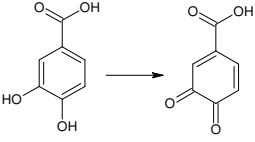
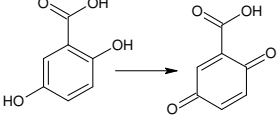
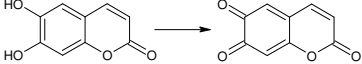
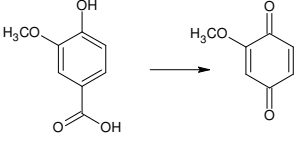
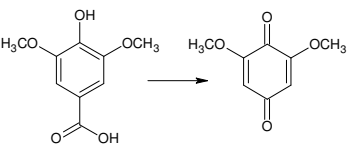
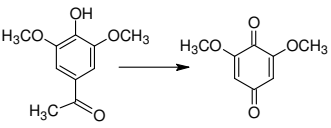
Results and Discussion

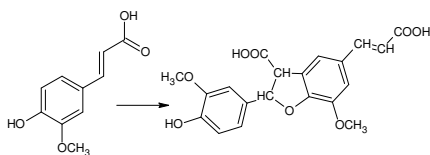
Normalization of ESI responses to obtain reaction kinetic plots. Monitoring the reaction progress was done using positive and negative ionization mode ESI simultaneously during the experiment. The aromatic amines could be detected better (STZ) or exclusively (EXA and ANL) in positive ionization mode and the phenols and dimers of phenolic precursors better in negative ionization mode. In negative mode signal responses (arbitrary units) were in general more than an order of magnitude lower than those in positive mode. Consequently, the signal responses from negative ESI would have been hardly visible on the same scale as those from positive ESI. Thus, detector responses were normalized in a first step to that of the aromatic amine educt for the positive ion mode and that of the phenol educt for the negative ion mode, yielding a response ratio. In a second step, the response ratios were normalized for the measured concentrations for the aromatic amines and phenols, respectively, which were derived by external calibration from the direct infusion of single solute aromatic amine and phenol standards. This yielded the normalized responses for all compounds monitored, which are shown in Figures 2, S7 and S8.

Tentative structure elucidation of reaction products by HRMS. For the reaction of STZ with CAT, 4mCAT, PRO, and GEN in the presence of laccase 1,4-reaction products were identified and their structures were tentatively assigned as shown in Figure S1-S4. The details for the assignment are given for the reaction of STZ with 4mCAT in the presence of laccase (Figure S2A), which resulted in the formation of one predominant reaction product, for which a monoisotopic mass of 375.0347 Da could be determined based on positive and negative ion HRMS ($[M-H]^-$ at m/z 374.0273, Figure S2A; $[M+H]^+$ at m/z 376.0419). The predicted molecular formula $C_{16}H_{13}O_4N_3S_2$ corresponded tentatively to the 1,4 addition product of STZ and 4mCAT, which was reoxidized to an anilinoquinone structure. The MS/MS fragmentation yielded characteristic product ions as shown in Figure S2B. The ions at m/z 123.0454 and m/z 254.0060 in the full scan mass spectra corresponded to unreacted 4mCAT and STZ, respectively. Less intense ions were observed in full scan mass spectra corresponding tentatively to reaction products containing two and three 4mCAT units and one STZ unit. In the short-term kinetic assay, these products emerged at later reaction times as compared to the STZ:4mCAT 1:1 reaction product, for which the intensity slightly decreased from 1000 s reaction time onwards (Figure S7). Due to their low intensity, no MS/MS spectra could be recorded. For the STZ:4mCAT 1:2 product, two principal tentative structures are possible, either a linkage of the STZ aniline nitrogen to both 4mCAT molecules or a linkage of the STZ aniline nitrogen to a 4mCAT dimer.

For the reaction of STZ with SYR, AcSYR and VAN in the presence of laccase 1,2-nucleophilic addition products were identified, as shown in Figure S5 and S6. HRMS spectra revealed the formation of 1,2-nucleophilic addition products, as exemplified for SYR in Figure S6A ($M-H$ at m/z 404.0369). The less intense ion at m/z 333.0604 with a molecular formula of $C_{16}H_{14}O_8$ corresponded probably to a SYR dimer, for which a structure was suggested by Leonowicz *et al.*⁵ The reaction pathway involves the oxidation of SYR by laccase through decarboxylation to 2,6-dimethoxy benzoquinone and the carbonyl C is attacked in a 1,2-addition reaction, followed by the elimination of water (imine formation).

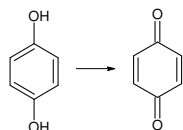
Table S2. Model humic constituents used to study NER formation mechanisms and reaction pathways proposed in this study. For hydroxyphenols, the oxidation reaction to the corresponding reactive quinone is shown; non-quinone carbonyl compounds are directly susceptible to nucleophilic addition reactions.

Phenols/Quinones	Names, Abbreviations, Standard reduction potentials (pH 7) E_h^0 , Initial mechanism
	<p>Catechol (CAT), 0.390 V^{Ref.6} Rapid¹ Michael addition of STZ, EXA, and ANL</p>
	<p>4-Methylcatechol (4mCAT), E_h^0 - no reference found Rapid Michael addition of STZ, EXA, and ANL</p>
	<p>Protocatechuic acid (PRO), 0.470 V^{Ref.6} Rapid Michael addition of STZ and EXA</p>
	<p>Gentisic acid (GEN), 0.356 V^{Ref.7} Rapid Michael addition of STZ and EXA</p>
	<p>6,7-Dihydroxycoumarin (esculetin, ESC), E_h^0 - no reference found No³ reaction of STZ and EXA with the formed quinone</p>
	<p>Vanillic acid (VAN), 0.181 V^{Ref.8} Rapid Schiff base formation to VAN dimers and small fraction of Michael addition to monomers of STZ and EXA</p>
	<p>Syringic acid (SYR), 0.101 V^{Ref.6} Rapid Schiff base formation of STZ, EXA, and ANL</p>
	<p>Acetosyringone (AcSYR), 0.101 V^{Ref.6} Rapid Schiff base formation of STZ and EXA</p>



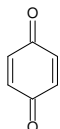
Ferulic acid (FER), E_h^0 - no reference found

No reaction with STZ and EXA, oligomerization products of FER observed^{Refs.9,10}



Hydroquinone (HQ), 0.286 V^{Ref.6}

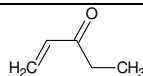
Slow² Michael addition of STZ and EXA after oxidation to p-benzoquinone, addition reaction is rate limiting; rate for EXA > STZ



p- Benzoquinone (BQ), 0.286 V^{Ref.6}

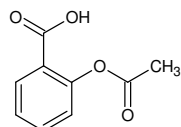
Slow Michael addition; reaction rate of EXA > STZ

Non-quinone carbonyl compounds



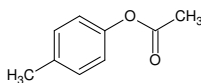
1-Penten-3-one

Slow Michael addition; reaction rate of EXA > STZ



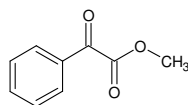
Acetylsalicylic acid

No reaction after 76 days



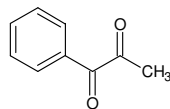
Acetic acid p-tolyl ester

No reaction after 76 days



Methylbenzoylformate

No reaction after 76 days



1-Phenyl-1,2-propanedione

No reaction after 76 days

¹Rapid reaction: conversion of aromatic amines > 60% within 30 minutes

²Slow reaction: conversion of aromatic amines > 20% within 2-76 days

³No reaction: = conversion of aromatic amines < 10% within 76 days, no reaction products detected by MS

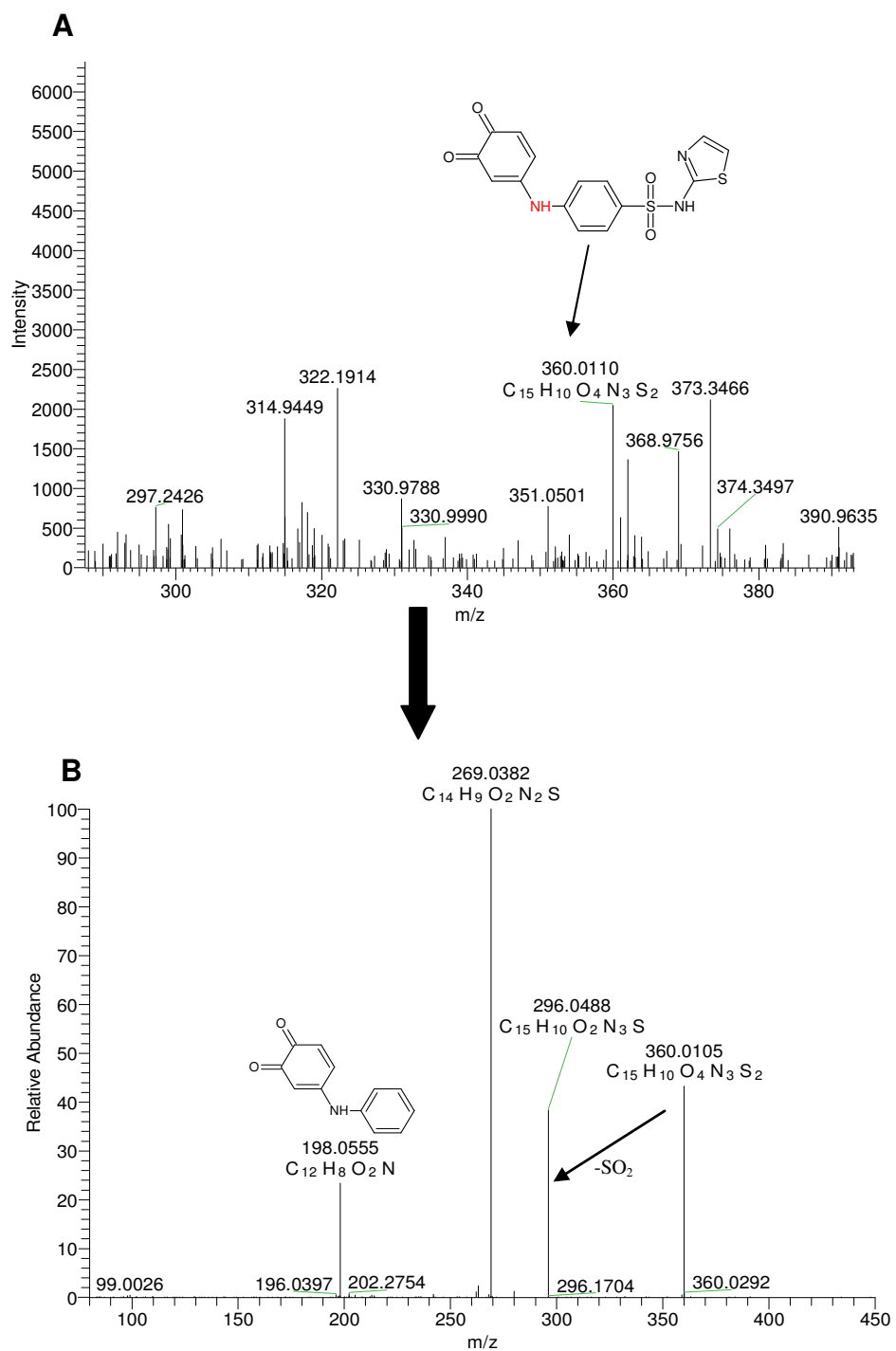


Figure S1: (A) High-resolution full scan mass spectrum (negative mode) of the reaction mixtures between sulfathiazole and catechol. (B) High resolution MS/MS product ion spectrum of the 1,4-nucleophilic addition product of sulfathiazole with catechol (m/z 360.0110).

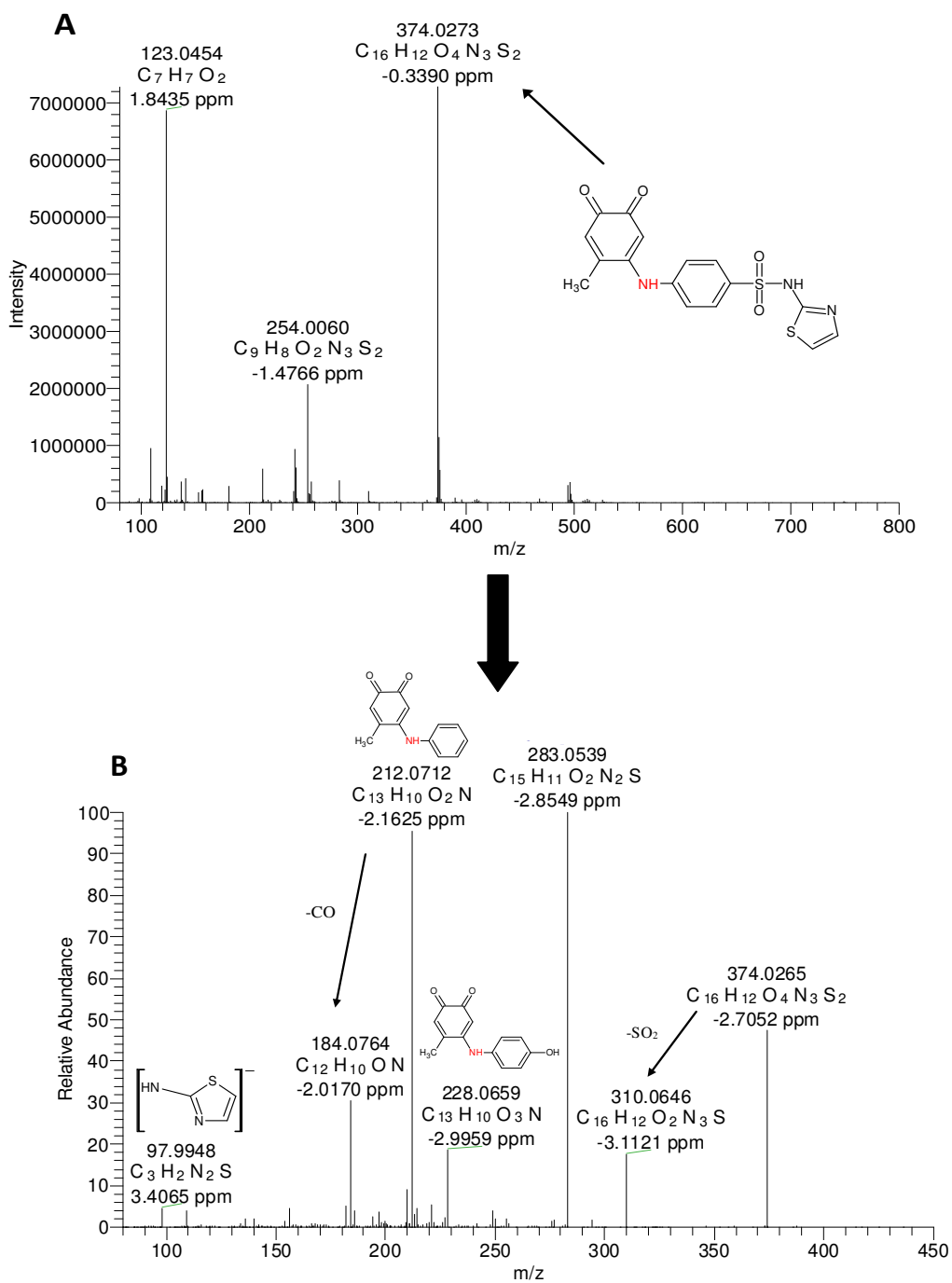


Figure S2: (A) High-resolution full scan mass spectrum (negative mode) of the reaction mixtures between sulfathiazole and 4-methylcatechol. (B) High resolution MS/MS product ion spectrum of the 1,4-nucleophilic addition product of sulfathiazole with 4-methylcatechol (m/z 374.0273).

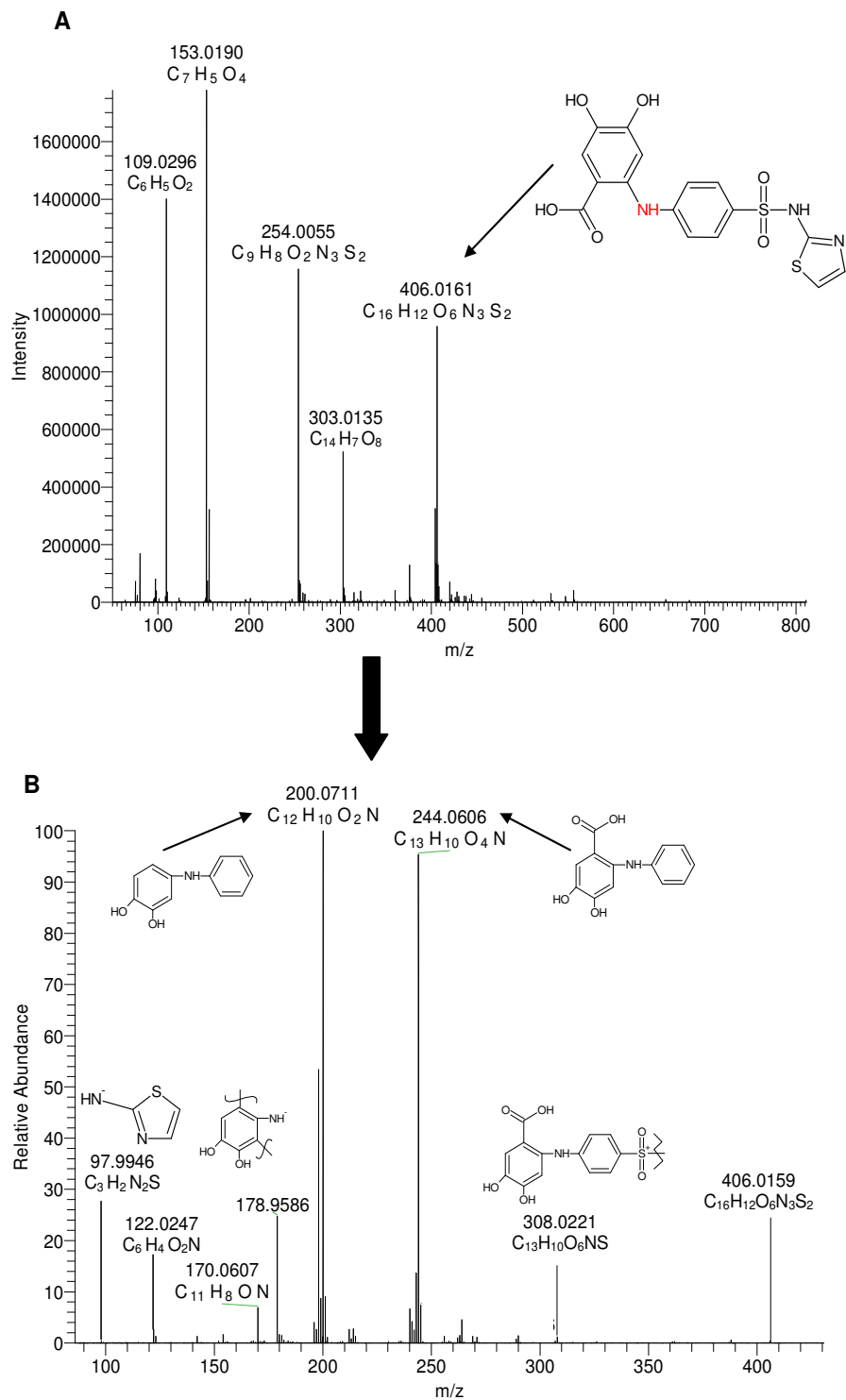


Figure S3: (A) High-resolution full scan mass spectrum (negative mode) of the reaction mixtures between sulfathiazole and protocatechuic acid. (B) High resolution MS/MS product ion spectrum of the 1,4-nucleophilic addition product of sulfathiazole with protocatechuic acid (m/z 406.0161).

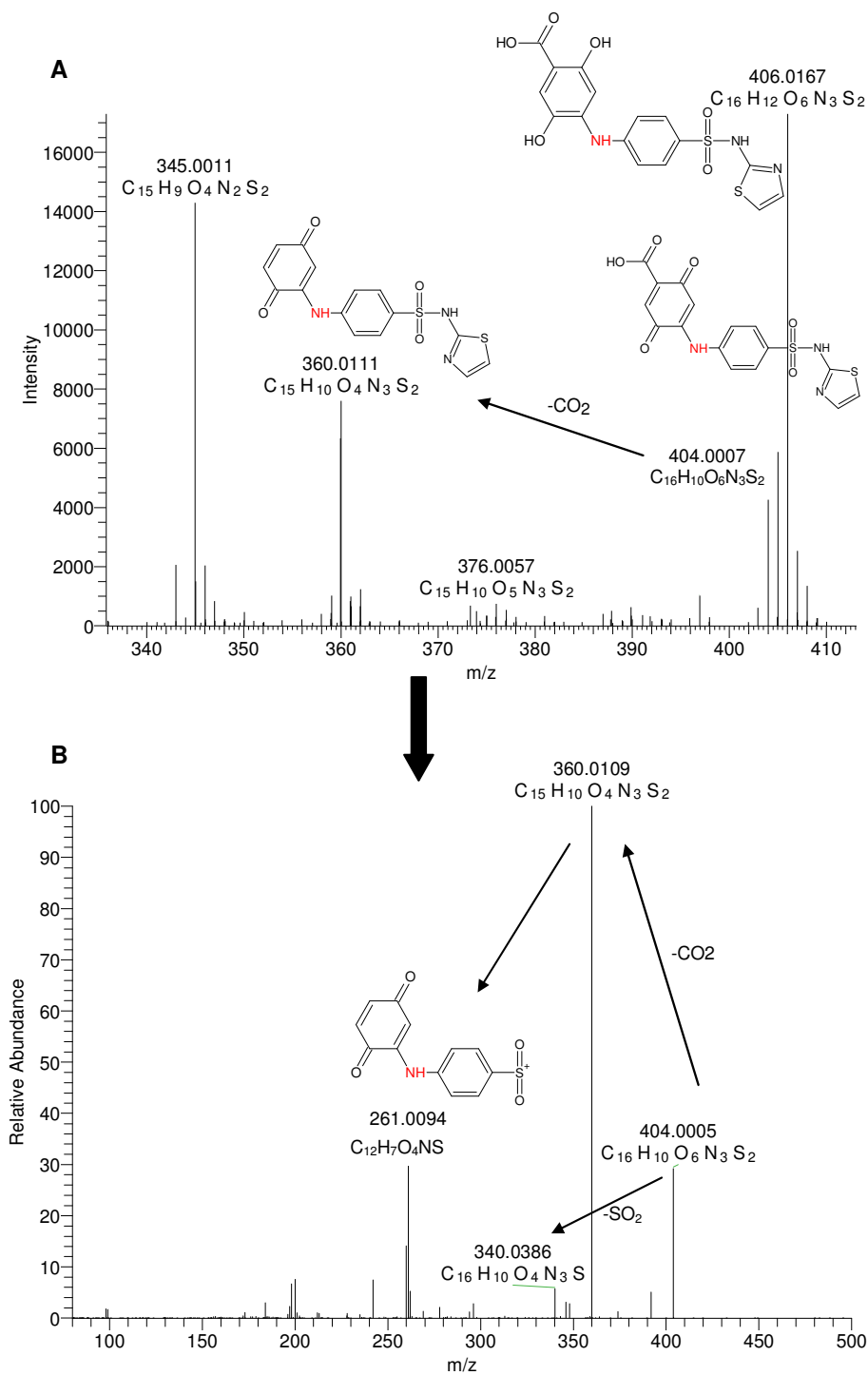


Figure S4: (A) High-resolution full scan mass spectrum (negative mode) of the reaction mixtures between sulfathiazole and gentisic acid. (B) High resolution MS/MS product ion spectrum of the 1,4-nucleophilic addition product of sulfathiazole with gentisic acid (m/z 404.0005).

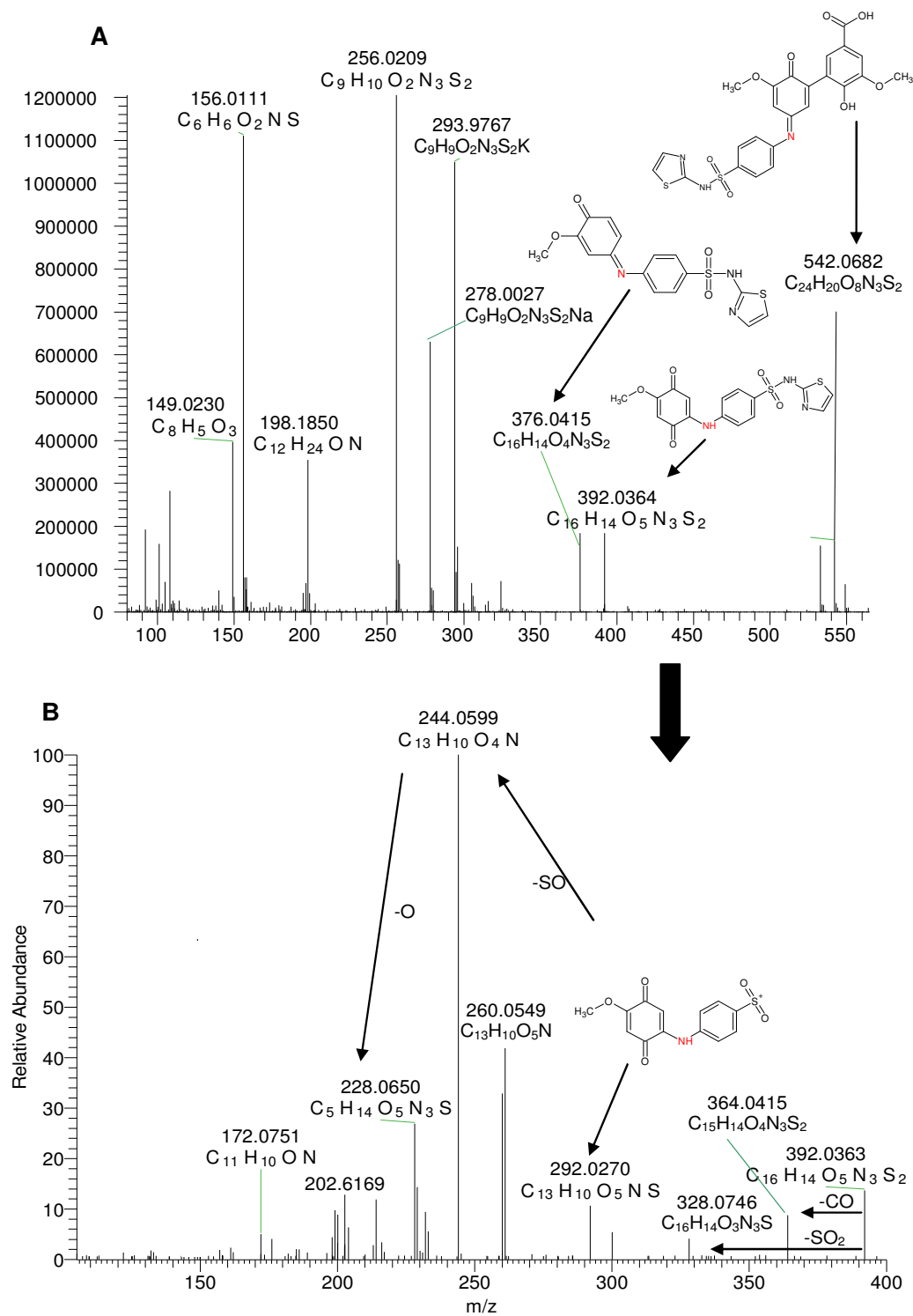


Figure S5: (A) High-resolution full scan mass spectrum (positive mode) of the reaction mixtures between sulfathiazole and vanilic acid. (B) High resolution MS/MS product ion spectrum of the 1,4-nucleophilic addition product of sulfathiazole with vanilic acid (m/z 392.0364).

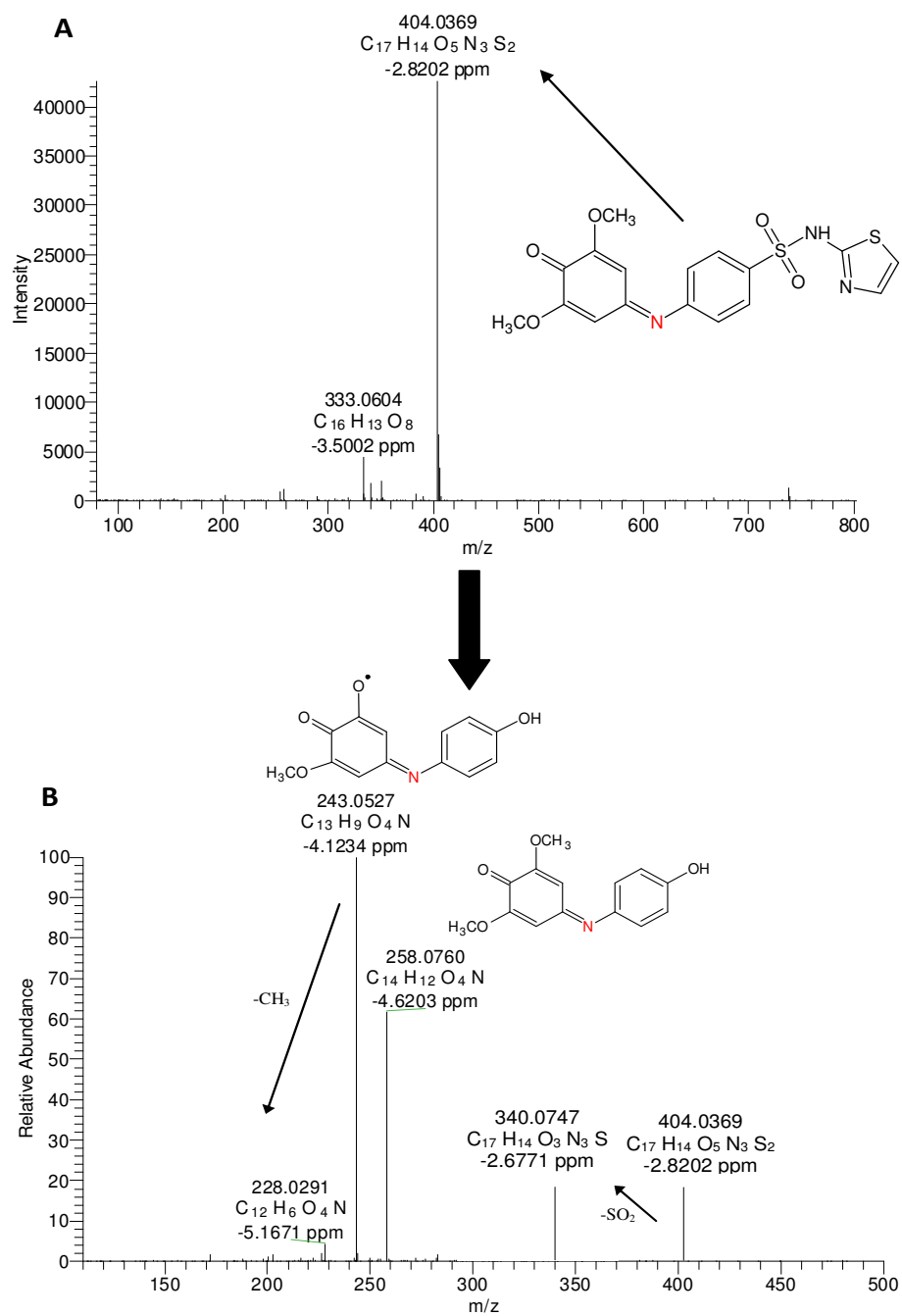


Figure S6: (A) High-resolution full scan mass spectrum (negative mode) of the reaction mixtures between sulfathiazole and syringic acid. (B) High resolution MS/MS product ion spectrum of the 1,2-nucleophilic addition product of sulfathiazole with syringic acid (m/z 404.0369).

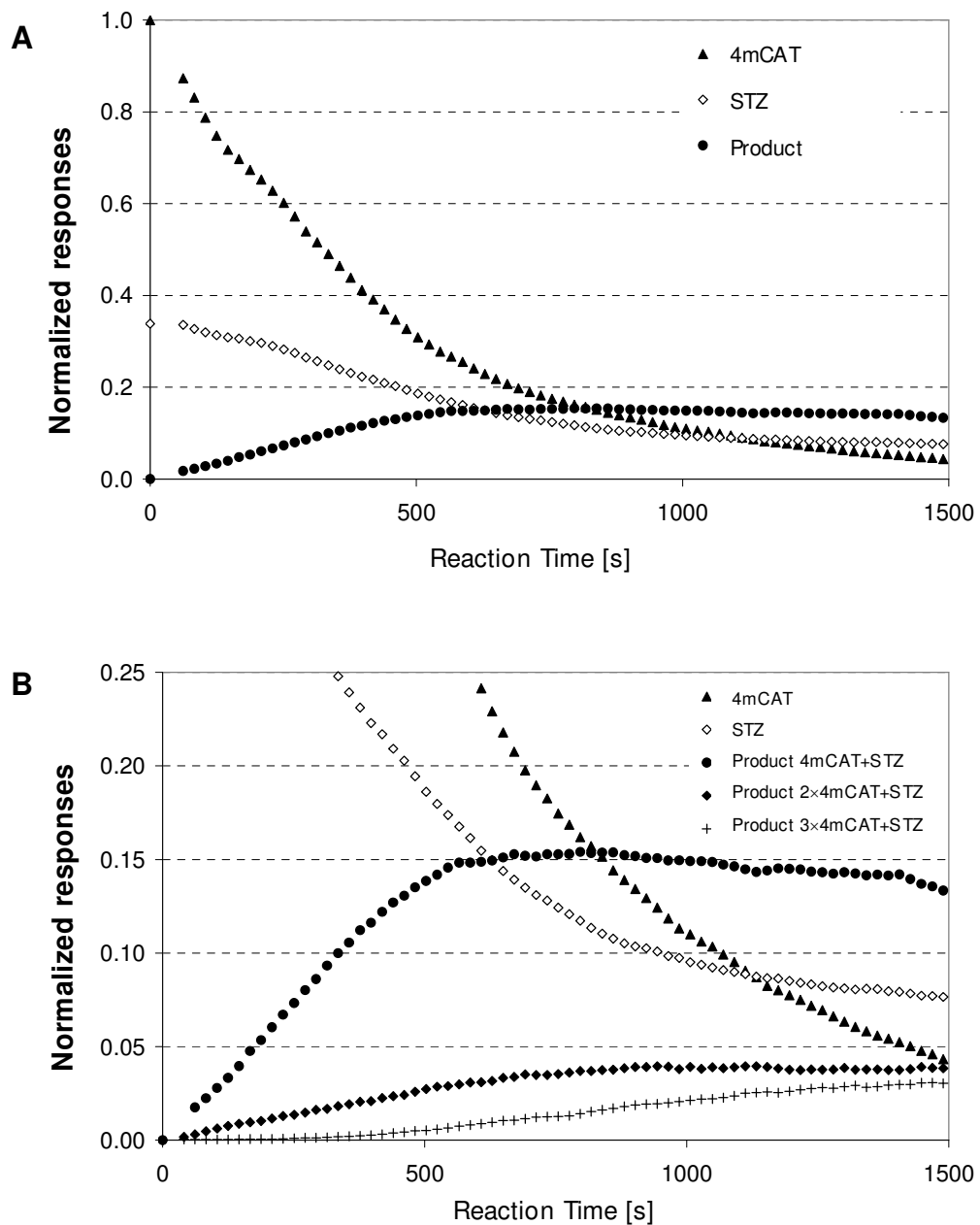


Figure S7: (A) Short-term kinetic assay of the reaction of sulfathiazole with 4-methylcatechol in the presence of laccase. Molar concentrations were normalized to 4mCAT for comparison. (B) Enlargement of the same kinetic assay showing oligomerization products. For the calculation of normalized responses see above (page S5).

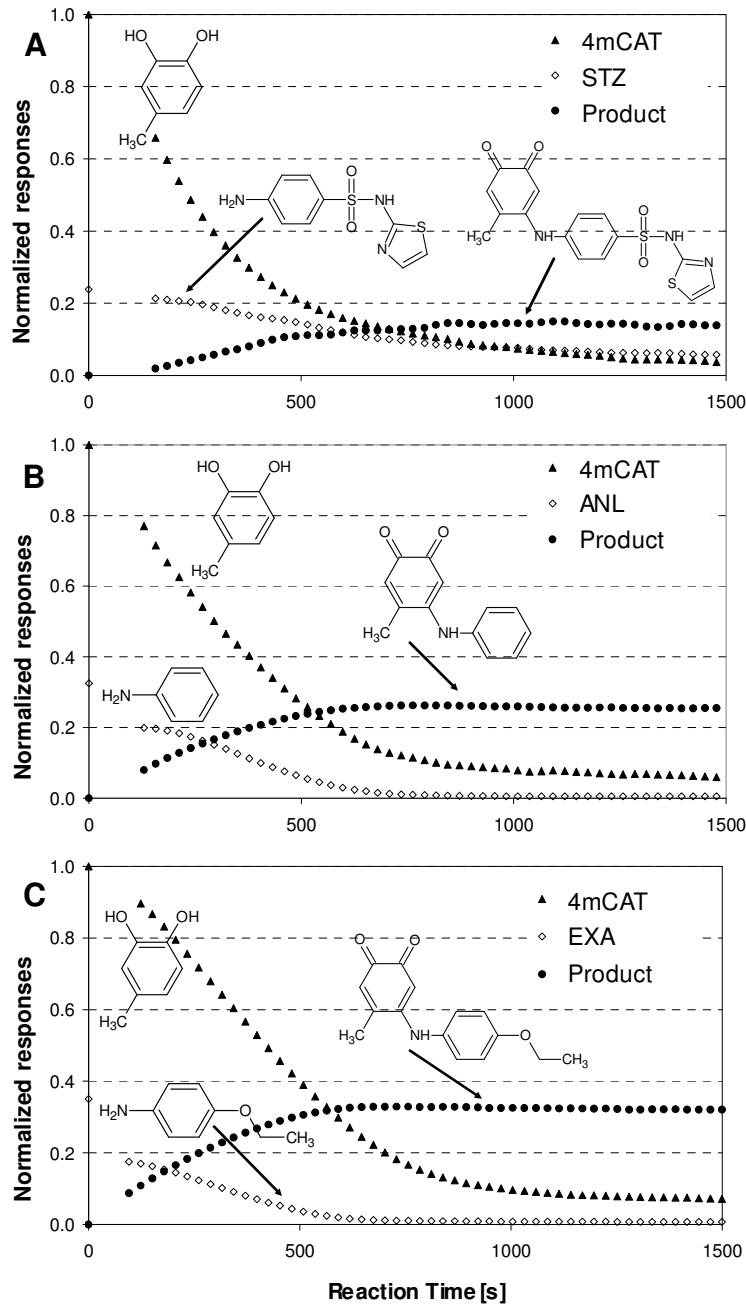


Figure S8: Short-term kinetic assays of the reaction of 4-methylcatechol with aromatic amines (A) sulfathiazole, (B) aniline, and (C) *p*-ethoxyaniline in the presence of laccase and 10-fold molar excess of *tert*-butanol. Molar concentrations were normalized to that of 4-methylcatechol for comparison. For the calculation of normalized responses see page S5.

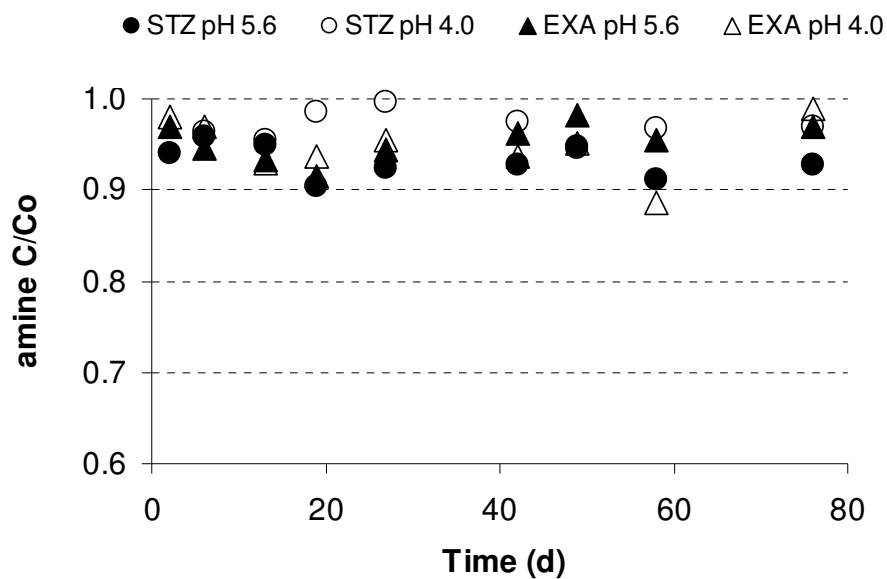


Figure S9: Control samples in the long-term kinetic assays containing only aromatic amine: sulfathiazole (STZ) and ethoxyaniline (EXA) in acetate buffer incubated over 76 days at two different pH values.

¹H and ¹⁵N NMR analysis of ¹⁵N aniline reaction products with CAT. The temporal changes in laccase-mediated reaction systems of ¹⁵N aniline-catechol and ¹⁵N aniline-syringic acid were monitored by ¹H-¹⁵N HMBC NMR spectra. In both systems the correlation signals from both, reacted and unreacted aniline were observed. Two aromatic protons ($\delta^1\text{H}$ at 6.7 and 7.0 ppm) of unreacted aniline correlated with the nitrogen at 58 ppm. The 2-hour long incubation of aniline with catechol and laccase yielded three major correlations to nitrogens with main resonances $\delta^{15}\text{N}$ at 101, 109, and 317 ppm (Figure 5a, see main text). The reaction product of STZ with CAT in the presence of laccase was identified earlier as an anilinoquinone (see main text). Anilinoquinone formation was reported in the reaction of aniline with humic substances based on tentative peak assignment in the $\delta^{15}\text{N}$ range of 100-122 ppm.⁴ Thus, the resonances at 101 and 109 ppm were assigned primarily to two different types of anilinoquinones. Although the $\delta^{15}\text{N}$ range of aromatic amides overlaps with those of anilinoquinones (100-110 ppm), a nucleophilic acyl substitution resulting in an amide bond is unlikely due to lack of carbonyl compounds in the aniline-catechol reaction system. The third resonance at 317 ppm mentioned above is in a typical range of chemical shifts for imines.¹¹ Simmons *et al.*¹² assigned this signal to an iminodiphenoquinone nitrogen observed in a product mixture obtained from the laccase-catalyzed reaction of guaiacol with 4-chloroaniline. The ¹⁵N chemical shifts of quinoline are normally expected in the same spectral region as those of imines. Owing to the absence of correlations to aromatic protons around $\delta^1\text{H} \approx 8.5 - 9.5$ ppm (expected from ¹H chemical shift calculations) the presence of this class of compounds is rather unlikely.

Significant changes in nitrogen chemical shifts (range of 0-200 ppm) were observed after longer incubation times of 2 hours to 20 days, with a significant increase of the signal of anilinoquinones at 101 and 109 ppm (Figure 5 a-b). A weak signal appeared at $\delta^{15}\text{N}$ 70 ppm corresponding to anilinohydroquinone. The resonances of anilinoquinone nitrogens are usually shifted to higher frequencies compared to those of anilinohydroquinones owing to a deshielding induced by deprotonation.¹³ The oxidative self-coupling of anilines may result in a wide range of products such as aminodiphenylamine, 1,2-diphenylhydrazine, benzidine, azobenzene, azoxybenzene.¹⁴ Phenazine and other diimine-derived structures reported by Simmons *et al.* may also occur in the region of imine nitrogens.^{12,15} The signal observed at $\delta^{15}\text{N}$ 95 ppm could correspond to hydrazine adducts, which serve as precursors in azobenzene formation. However, we observed no correlations that could possibly be assigned to azobenzenes in the recorded spectra. Thorn *et al.*¹⁴ reported that the kinetically controlled reaction of aniline with fulvic acid

was favored over coupling with aniline itself in the presence of peroxidase. Thus, we assume that the contribution of self condensation products of aniline to the spectra is negligible.

We were unable to assign the signals at $\delta^{15}\text{N}$ 162 ppm. A tentative assignment reported by Thorn *et al.*⁴ suggests that this resonance may correspond to pyrroles, indoles or similar heterocyclic nitrogens.

New correlations were observed also in the region of imine nitrogens around 320 and 338 ppm. Possible assignments of these resonances could include quinoline or phenazine nitrogens and in fact, phenazines have been reported to appear in early stage of aniline oxidation.¹⁵ The weak signal at $\delta^{15}\text{N}$ 331 ppm may be assigned to quinone imines or iminediphenoquinones.⁴

The ^1H - ^{15}N HMBC NMR experiment of the 20 day sample was analyzed again after 60 days of storage in solution. Some NaOD solution was added to fully dissolve the sample. A significant new signal was observed at $\delta^{15}\text{N}$ 196 ppm (Figure 5c). At the same time the relative intensities of both, anilinoquinones and imines, significantly decreased. The outstanding resonance at 196 ppm may be assigned to imidazoles or benzimidazoles.¹⁶ With continuing incubation time the relative signal intensity of the aniline nitrogen resonance continuously decreased and in the spectrum recorded after 2 months the major signal was observed in the region of heterocyclic nitrogens.

^1H and ^{15}N NMR analysis of ^{15}N aniline reaction products with SYR. Incubation of aniline with syringic acid and laccase yielded correlation signals in the ^1H - ^{15}N HMBC NMR spectra that indicate covalent bond formations (Figure S10a). A weak resonance at $\delta^{15}\text{N}$ 103 ppm was assigned to anilino-1,4-quinone nitrogens. As already reported for the catechol incubation experiments we also observed a strong correlation at 338 ppm assigned to imines. The 1,2-addition of aniline nitrogen to sterically hindered quinones results in quinone imine formation (Schiff bases). As reported earlier the reaction of STZ with SYR in the presence of laccase resulted in the formation of imines following the 1,2 addition reaction pathway. We assume a similar mechanism for aniline but, unfortunately, adequate chemical shift references for deprotonated quinone imines are difficult to obtain.¹⁷ However, the tentative assignment of $\delta^{15}\text{N}$ 338 ppm to quinone imines reported by Thorn *et al.*⁴ reasonably fits to our results. In this chemical shift region also the nitrogens of phenoxazinones are expected. However, we did not observe any correlations to highly deshielded protons expected from ^1H chemical shift calculations for this class of compounds. The weaker correlation signals observed in the spectral region of imines ($\delta^{15}\text{N} \approx 350$ ppm) may originate of hydrazones or oximes.

As observed for the incubation of catechol, the distribution of nitrogen changed with time in the syringic acid series. After 2 days of incubation, significantly increased resonances

corresponding to anilinoquinones were observed (Figure S10b). In contrast to the reaction carried out in the presence of catechol, the resonance at 70 ppm assigned to anilinohydroquinones did not appear in this series of spectra during the entire incubation time. Additionally to the quinone imines ($\delta^{15}\text{N}$ 338 ppm), new signals at 321 and 354 ppm indicated the presence of hydrazones and oximes, respectively. The weak signal at 344 ppm may originate from azoxybenzenes, also explaining the presence of a new weak correlation observed at 95 ppm assignable to hydrazines. No significant deviations of relative signal intensities were noticed between day 2 and 5 (Figures S10 b and c). After 20 days, however, the resonance of the quinone imine at 338 ppm decreased beyond the detection limit, whereas a new resonance at 145 ppm appeared in the region assigned to anilides, enaminones, quinolones and/or indoles by Thorn *et al.*⁴

Figure S10 e shows the ^1H - ^{15}N HMBC NMR spectrum of the reaction mixture of the day 20 sample re-measured after 4 weeks in solution. The signals of hydrazones at 321 and anilinoquinones at 100 ppm significantly decreased. Instead, two major resonances corresponding to free (unreacted or released) aniline at 58 ppm and a new signal of anilide or acetanilide nitrogens at 125 ppm were observed. The signal at 127 ppm may correspond to enaminones.⁴

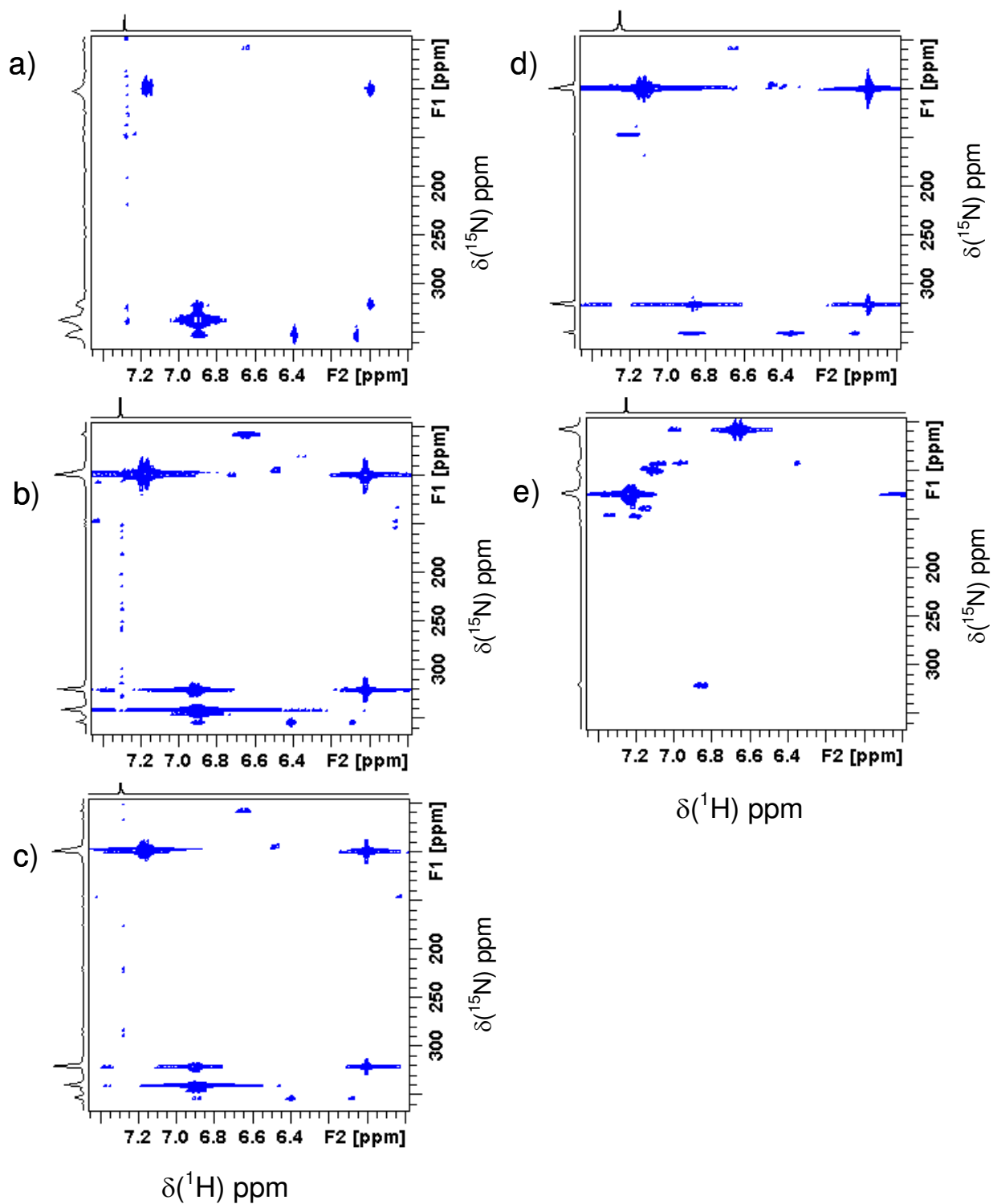


Figure S10: ^1H - ^{15}N HMBC NMR spectra of ^{15}N -aniline transformed in presence of syringic acid and laccase after a) 2 hours, b) 2, c) 5 and d) 20 days of incubation. Spectrum e) was recorded after storing the solution for additional 30 days at room temperature.

References

1. Richter, M. K.; Sander, M.; Krauss, M.; Christl, I.; Dahinden, M. G.; Schneider, M. K.; Schwarzenbach, R. P. Cation Binding of Antimicrobial Sulfathiazole to Leonardite Humic Acid. *Environ. Sci. Technol.* **2009**, *43*, (17), 6632-6638.
2. Mackay, D.; Shiu, W. Y.; Ma, K.-C.; Lee, S. C. *Handbook of Physical-Chemical Properties and Environmental Fate for Organic Chemicals, Second Edition*. CRC Press: Boca Raton 2006; p 4182.
3. Anslyn, E. V.; Dougherty, D. A. *Modern Physical Organic Chemistry*. University Science Books: Sausalito, 2006.
4. Thorn, K. A.; Pettigrew, P. J.; Goldenberg, W. S. Covalent binding of aniline to humic substances. 2. ^{15}N NMR studies of nucleophilic addition reactions. *Environ. Sci. Technol.* **1996**, *30*, (9), 2764-2775.
5. Leonowicz, A.; Edgehill, R. U.; Bollag, J. M. The Effect of Ph on the Transformation of Syringic and Vanillic Acids by the Laccases of *Rhizoctonia-Praticola* and *Trametes-Versicolor*. *Arch. Microbiol.* **1984**, *137*, (2), 89-96.
6. Clark, W. M. *Oxidation-reduction potentials of organic systems*. The Willimas & Wilkins Company: Baltimore, MD, 1960.
7. Pelizzetti, E.; Mentasti, E.; Baiocchi, C. Kinetics and mechanism of oxidation of quinols by hexachloroiridate(IV) in aqueous acidic perchlorate media. *J. Phys.Chem.* **1976**, *80*, (27), 2979-2982.
8. Clemmer, J. D.; Hogaboom, G. K.; Holwerda, R. A. Reduction of the bis(2,9-dimethyl-1,10-phenanthroline)copper(II) ion by substituted hydroquinones. *Inorg. Chem.* **1979**, *18*, (9), 2567-2572.
9. Carunchio, F.; Crescenzi, C.; Girelli, A. M.; Messina, A.; Tarola, A. M. Oxidation of ferulic acid by laccase: identification of the products and inhibitory effects of some dipeptides. *Talanta* **2001**, *55*, 189-200.
10. Tatsumi, K.; Freyer, A.; Minard, R. D.; Bollag, J. M. Enzyme-Mediated Coupling of 3,4-Dichloroaniline and Ferulic Acid - a Model for Pollutant Binding to Humic Materials. *Environ. Sci. Technol.* **1994**, *28*, (2), 210-215.
11. Simmons, K. E.; Minard, R. D.; Bollag, J. M. Oxidative co-oligomerization of guaiacol and 4-chloroaniline. *Environ. Sci. Technol.* **1989**, *23*, (1), 115-121.
12. Simmons, K. E.; Minard, R. D.; Bollag, J. M. Oligomerization of 4-Chloroaniline by Oxidoreductases. *Environ. Sci. Technol.* **1987**, *21*, (10), 999-1003.
13. Bialk, H. M.; Pedersen, J. A. NMR Investigation of Enzymatic Coupling of Sulfonamide Antimicrobials with Humic Substances. *Environ. Sci. Technol.* **2008**, *42*, (1), 106-112.
14. Thorn, K. A.; Goldenberg, W. S.; Younger, S. J.; Weber, E. J. Covalent Binding of Aniline to Humic Substances. In *Humic and Fulvic Acids*, American Chemical Society: 1996; Vol. 651, pp 299-326.
15. Sapurina, I.; Stejskal, J. The mechanism of the oxidative polymerization of aniline and the formation of supramolecular polyaniline structures. *Polym. Int.* **2008**, *57*, (12), 1295-1325.
16. Berger, S.; Braun, S.; Kalinowski, H.-O. *NMR Spectroscopy of the Non-Metallic Elements*. Wiley: 1997.

17. Bialk, H. M.; Simpson, A. J.; Pedersen, J. A. Cross-coupling of sulfonamide antimicrobial agents with model humic constituents. *Environ. Sci. Technol.* **2005**, *39*, (12), 4463-4473.